

Investigation of C V line ratio variations in a tokamak with an application to neutral hydrogen measurement

K. J. McCarthy, B. Zurro, C. Burgos, J. Vega, and A. Portas

Asociación EURATOM/CIEMAT para Fusión, Avenida Complutense 22, E-28040 Madrid, Spain

(Received 16 May 1995; revised manuscript received 7 August 1995)

Significant differences in the ratio between the He-like carbon triplet lines $1s2s\ ^3S_1-1s2p\ ^3P_2$ (2271.59 Å) and $1s2p\ ^3S_1-1s2p\ ^3P_{0,1}$ (2278.41 Å) have been observed in line of sight measurements across the *TJ-I* tokamak. Such variations, which deviate from the $2\ ^3P$ level statistical ratios, have not been reported for this line ratio in similar fusion plasmas. We show that such differences can be explained by charge exchange, involving collisions between H-like carbon ions and neutral hydrogen atoms, while ruling out excitation and deexcitation by electron collisions and line blending effects. Finally we discuss similar transitions in other low Z ions and propose monitoring these variations as a spectroscopic tool for estimating relative neutral concentrations in plasmas.

PACS number(s): 52.70.Kz, 34.70.+e, 34.80.Dp

I. INTRODUCTION

This work is prompted by the need to understand significant variations in the ratio of the intensities of the important He-like carbon (C V) triplet emission lines $1s2s\ ^3S_1-1s2p\ ^3P_{2,0,1}$ with wavelengths 2271.59, 2277.97, and 2278.63 Å [1], which were observed in line of sight measurements across the *TJ-I* tokamak plasma. The emissions, which are the result of the radiative decay of the triplet $2\ ^3P$ levels, are widely used in studies of many He-like low Z ions [2,3], while information on the electron temperature and density of both astrophysical and laboratory plasmas is generally ascertained by measurement of the intensity ratios of these and other associated transitions [4,5]. While similar anomalies have not been reported previously for these line ratios, one reason being that such observations are generally not spatially resolved [6], it is interesting to note that significant variations have been observed in the ratios of lines that emanate from the same $2\ ^3P$ levels. For instance, variations have been reported in the ratio of the intercombination lines $1s^2\ ^1S_0-1s2p\ ^3P_{2,1}$ of both He-like sulfur (S XV) and He-like chlorine (Cl XVI) in measurements across the Alcator-C tokamak [7]. In addition, significant variations have also been seen in the G ratio (i.e., intercombination to resonance line ratio) of spatially resolved C V line emissions taken across the Tore Supra tokamak [8]. Since these tokamaks are similar in many respects to the *TJ-I* tokamak, there is reason to believe that there exists a common source for these anomalies.

From the literature, several candidates have been found that might account for these variations. The first and most obvious is contamination of the lines by emissions from other ion species in the plasma. Systematic checks through the standard reference tables [9,10] show that no other low Z lines are within ± 0.5 Å of the carbon triplet lines. In a paper on hot θ -pinch plasmas, Engelhardt, Köppendörfer, and Sommer [11] report significant variations in the ratios of the same transitions in He-like oxygen (O VII). They show how competing ra-

diative decays and electron excitations to the excited levels can combine to give rise to such variations, but when their model is extrapolated to the lower electron densities of the *TJ-I* experiment, typically less than 5×10^{13} cm⁻³, the C V line ratios are constant across the plasma and in accordance with the statistical weights of the various levels. Chung, Lemaire, and Suckewer [12] hypothesize that the spontaneous emission coefficients are not constant for levels but can change with electron density. However, for such a change to occur in any of the C V $2\ ^3P$ level spontaneous emission coefficients, the electron density should be from several to many orders of magnitude greater than those experienced here. The other candidate considered is charge exchange (CX) [13], where electrons, which are state selectively captured by multiply charged impurity ions during collisions with neutral atoms, decay to selectively populate lower levels. Despite the low concentration of neutral atoms found in fusion plasmas, we believe that CX can compete with electron collisions, which populate the $2\ ^3P$ levels according to their statistical weights, to create a nonstatistical population distribution among these levels. This is because the cross sections for CX, which can be of the order 10^{-15} cm², are much larger than those of other atomic collision processes. Using equations developed to include CX contributions, we model the $2\ ^3P$ line emissions and compare model results for C V with measured results to demonstrate that CX between neutral atoms and H-like carbon (C VI) ions has caused the anomalies observed.

II. EXPERIMENTAL APPROACH

The measurements reported here were made on the *TJ-I* tokamak. The *TJ-I* plasma has a major radius of 30 cm and a minor radius of 10 cm. The machine was operated for this experiment with plasma currents around 40 kA, a toroidal field of 1.2 T, and line averaged electron densities between 2 and 2.5×10^{13} cm⁻³. The machine is described in more detail by Zurro *et al.* [14]. Line of sight UV measurements through ohmically heat-

ed discharges were made between 2250 and 2310 Å by using a 1 m focal length monochromator with spatial and temporal resolution capabilities. The spectra were recorded by using a commercial multichannel intensified detector with 700 active pixels mounted at the monochromator focal plane. With the detector operating in gated mode, line emissions were integrated for 4–6 ms, this period being centered about the peak of the discharge. Optical access to the entire plasma was possible by using a rectangular quartz window on the machine. The light from the plasma was rotated through 90° by a set of three mirrors positioned close to the window. This light was then focused onto the monochromator slit ($5 \times 0.1 \text{ mm}^2$) by a lens. A standard lamp was used for calibration and alignment. Rotation of the mirror closest to the quartz window was controlled electronically, allowing the optical line of sight through the plasma to be varied on a shot to shot basis. This mirror was replaced by a fast rotating polygonal prisms to obtain line-integrated emission profiles. A personal computer was used to control the detector and to store data files. Postexperimental data processing and analysis were done on Vax and Macintosh computers.

A. Results

In Fig. 1, we show one of a series of line of sight raw spectra collected during one of several sets of *TJ-I* discharges. It shows that the C V emission lines, centered at 2271.59 and at 2278.41 Å, are clear of contamination lines, except for the Be-like carbon (C III) line at 2296.9 Å. Despite the use of a high resolution monochromator, the closely spaced C V emission lines at 2277.97 Å (from 2^3P_0) and at 2278.63 Å (from 2^3P_1) are not resolved. In Fig. 2(a), the variation in the intensity of the 2271.59 Å line (from 2^3P_2) across the plasma minor radius, with background subtracted, is shown for one complete set of discharges. These data were later used to determine the distribution of C V in the plasma. Note that the line of sight view was typically 1.5 cm.

In Fig. 2(b), the ratio of the line intensities $R = I(2271.59 \text{ Å})/I(2278.41 \text{ Å})$ shows significant variations across the plasma radius. The most dramatic is the sharp rise in R moving inward from the plasma edge, which is followed by a slow drop continuing to the

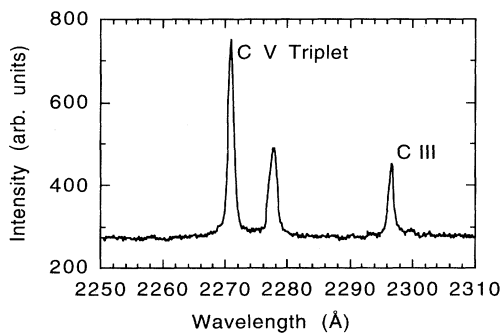


FIG. 1. Raw spectral data for a line of sight measurement through the *TJ-I* plasma.

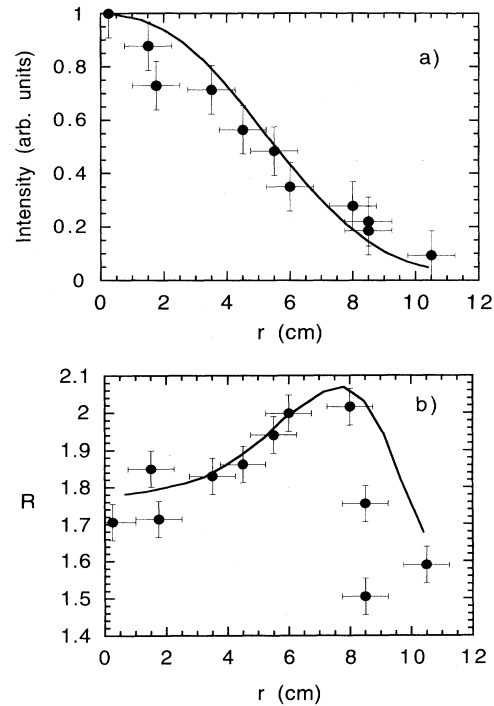


FIG. 2. (a) The 2271.59 Å line intensity and (b) the intensity ratio R of the 2271.59 Å and 2278.41 Å lines across the *TJ-I* plasma radius r for a series of discharges. The points are measured data and the curves are model results. The nonzero value at radius 10.4 cm in (a) is due to line of sight geometry.

center. These variations are much greater than the experimental errors, while R is significantly larger, except at the edge, than $R = 1.67$, predicted by extrapolating to the *TJ-I* conditions the formulas developed by Engelhardt *et al.* [11]. It is these variations together with similar variations seen in the other sets of discharges that are the basis of our studies here. In the following sections we review the physics involved in these line emissions and develop equations that are incorporated into a model to reproduce the results shown here.

III. DISCUSSION

Before discussing charge exchange and its role in populating the $n=2$ triplet levels, it is useful to review the other populating and depopulating mechanisms of low Z He-like ions. Although He-like ions exhibit a singlet and triplet term structure and line emissions over a wide range of wavelengths, it is the fine structure of the triplet manifolds 2^3P level and the associated radiative transitions shown in Fig. 3 that are of prime interest. The main decay mechanisms for these levels is via allowed $E1$ radiation to the metastable 2^3S_1 level, and since the differences in energy between these 2^3P levels are very small (for carbon, ΔE is 135.9 cm^{-1} between 2^3P_2 and 2^3P_1 and 123.3 cm^{-1} between 2^3P_2 and 2^3P_0 [1]), the lines from these transitions are often difficult to resolve. The spontaneous emission coefficient rates A_{km} , which are now well established for these decays, are also similar

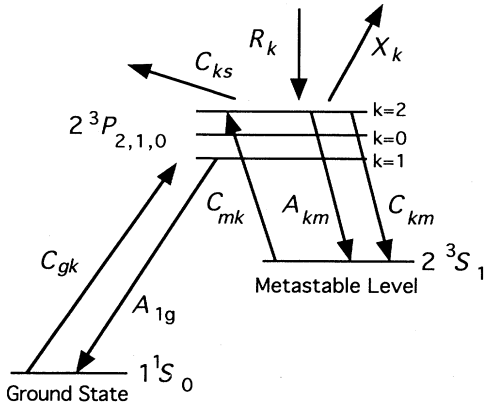


FIG. 3. Denotation of levels and transitions in C v. C_{gk} , C_{mk} , and C_{ks} refer to rate coefficients for excitations $1s\ ^1S_0-2p\ ^3P$, $2\ ^3S_1-2p\ ^3P$, and $2p\ ^3P-2s\ ^1S$ and $-2p\ ^1P$; R_k to rates for cascades; X_k to ionizing collision rates; C_{km} to deexcitation rates for $2p\ ^3P-2s\ ^3S_1$; and A_{km} and A_{1g} to transition probabilities for $2p\ ^3P_k-2s\ ^3S_1$ and for $2p\ ^3P_1-1s\ ^1S$.

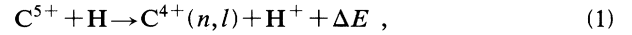
[3]. In contrast these levels decay to the atomic ground state $1\ ^1S_0$ by completely different modes, the $2\ ^3P_2$ state by $m2$ radiation, the $2\ ^3P_1$ state by spin-forbidden $E1$ radiation, and the $2\ ^3P_0$ state by two or three photon radiation. The first and last of these transition modes are too slow to compete in the depopulation process, while the second, which is compatible with the rates to $2\ ^3S_1$, competes to depopulate the $2\ ^3P_1$ level [3]. It is shown later that consideration of this decay route is not sufficient to explain the anomalies seen. Finally, several other processes also depopulate the $2\ ^3P$ levels. These include collisional deexcitation to the $2\ ^3S_1$ level C_{km} , ionizing collisions X_k , electron collisional excitations to higher states (predominantly into the 3D level), and spin exchange to the $2\ ^1P_1$ level C_{ks} . Their cross sections are generally much less than for other processes, but they are included here for completeness.

In contrast, the main population mechanism for these levels is electron collisional excitation from the ground $1\ ^1S_0$ state C_{gk} . According to Percival and Seaton [15], collisional excitation processes populate the $2\ ^3P$ levels in accordance with the statistical weights of the upper levels, i.e., 5 to 3 to 1 for $2\ ^3P_2$, $2\ ^3P_1$, and $2\ ^3P_0$. Note that electron induced collisional transitions between these fine structures can be neglected in any population models, as shown by Doyle [16]. The other processes normally considered to populate these levels are electron collisional excitation from the metastable $2\ ^3S_1$ level C_{mk} and cascades from higher triplet levels R_k . Of all these, only cascades do not populate the levels in accordance with the ratios above [17]. In plasmas such as the *TJ-I* plasma, where electron densities and temperatures are low, cascades due to electronic excitation of upper levels are generally weak, while those due to charge exchange have previously not been considered of importance in populating the $2\ ^3P$ levels. We now briefly describe charge exchange before developing equations to estimate the populations of the levels.

A. Charge exchange

Much work has been done to date on CX processes in plasmas involving collisions over a wide range of energies and between many species of highly stripped ions and neutral atoms and molecules. These studies are of great interest for plasma diagnostics because CX provides a means to detect, through charge exchange recombination spectroscopy, bare nuclei of low Z ions in the hot plasma center. Generally neutral hydrogen heating and diagnostic beams are used to excite the diagnostic spectral lines, but CX interactions involving the neutral hydrogen atoms that continuously recycle from the plasma edge can also excite such lines [18]. This is because these neutral hydrogen atoms can penetrate to the hot plasma center by diffusion from the edges through successive charge transfers with the working gas ions. As a result their densities can be from 10^8 to $10^{10}\ \text{cm}^{-3}$ at the plasma center, which are two to three orders of magnitude lower than at the periphery. Since neither diagnostic nor heating beams were used in our experiments, it is CX involving slow collisions between these recycling hydrogen atoms and H-like carbon ions that are of most interest.

This collision process is described by



where (n, l) is the capture state for the electron and ΔE is the excess energy. Those electrons captured by different l levels of high n states in the triplet manifold of the He-like ions cascade rapidly through the lower levels and states to the metastable level. Since electrons are captured into $n > 2$ states and certain interlevel transitions are forbidden, cascades from some levels decay only through the $2\ ^3P_2$ level and not the $2\ ^3P_1$ level [17]. Under favorable conditions, for example, when the neutral density is high enough, the resultant population in the $2\ ^3P_2$ level can be greater than that in either of the other two $2\ ^3P$ levels, thus giving rise to changes in the $2\ ^3P$ level emission line ratios. In the following section these arguments are expanded upon, and equations that include the charge exchange process are developed to estimate the steady state populations in each of the $2\ ^3P$ levels.

B. Level populations

The arguments and equations outlined here could in theory be applied to a range of low Z He-like ions, from B to Ne, but to avoid complicating the text we concentrate on the case of He-like carbon. In addition, for simplicity, several reasonable and well supported assumptions and approximations are made throughout the text. In an optically transparent plasma, the line intensity of a transition from one of the $2\ ^3P$ levels, k , to the metastable level, m , can be expressed as $I_{km} = A_{km}n_k$ ($\text{cm}^{-3}\ \text{s}^{-1}$), where A_{km} is the decay rate to the metastable. For low Z He-like ions, A_{km} are almost equal for the three $2\ ^3P$ levels [3,19], so the ratios of the line intensities I_{km} can be expressed in terms of n_k , the k level steady state population. That is to say, variations in intensity are directly attributable to variations in level populations. To determine n_k it is necessary to consider that the plasma is in a

steady state, i.e., $dn_j/dt=0$ for all levels, where the population n_j of any level j of the ion can be expressed in terms of its principal population and depopulation rates.

Many authors have described such equations, but we use the equation given by Keenan [5] as the basis for our work. It is modified here to include the level statistical weights, which is reasonable since electron collisions populate each level according to the upper level statistical weight, and to account for cascades from higher levels. Thus the steady state population n_k in the 2^3P_k level is given as

$$n_k = \frac{w_k \left[N_e \sum_{j=1}^n n_j C_{jk} \right] + R_k}{\sum_{j=1}^i A_{kj} + N_e \sum_{j=1}^n C_{kj}}, \quad (2)$$

where w_k is the k level statistical weight, C_{jk} and C_{kj} are the electron collisional rates into and out of the k level, A_{kj} is the radiative rate out of the same, N_e is the plasma local electron density, n_j is the j level population, and R_k is the cascade rate into the k level from higher levels. When this equation is applied to $TJ-I$ -like plasmas, electronic collisions into the 2^3P levels from the ground and metastable levels are included and the R_k term is split into two parts: R_k^* to account for cascade from dielectric and radiative recombination of the hydrogen-like ion and $N_0 N_h \sigma_k V_a$ to include those electrons that are captured during CX and decay through the 2^3P levels. Here N_0 is the plasma local neutral density (cm^{-3}), N_h is the H-like ion local density (cm^{-3}), σ_k is the k level cascade corrected emission cross section for CX (cm^2), and V_a is the relative ion-neutral collision velocity (cm s^{-1}). Finally, cascades that originate as electron excitations into states $n=3$ and 4 are considered minimal and are neglected. Therefore the steady state population in each k level is estimated, for the local electron temperature, by using

$$n_2 = \frac{\frac{5}{9} [N_e (n_g C_{g2} + n_m C_{m2})] + R_2^* + N_0 N_h \sigma_2 V_a}{\left[A_{2m} + N_e \sum_{j=1}^n C_{2j} \right]} \quad \text{for } k=2, \quad (3)$$

$$n_1 = \frac{\frac{3}{9} [N_e (n_g C_{g1} + n_m C_{m1})] + R_1^* + N_0 N_h \sigma_1 V_a}{\left[A_{1m} + A_{1g} + N_e \sum_{j=1}^n C_{1j} \right]} \quad \text{for } k=1, \quad (4)$$

$$n_0 = \frac{\frac{1}{9} [N_e (n_g C_{g0} + n_m C_{m0})] + R_0^* + N_0 N_h \sigma_0 V_a}{\left[A_{0m} + N_e \sum_{j=1}^n C_{0j} \right]} \quad \text{for } k=0, \quad (5)$$

where $w_k = \frac{5}{9}$, $\frac{3}{9}$, and $\frac{1}{9}$ for 2^3P_2 , 2^3P_1 , and 2^3P_0 ; and A_{km} and A_{1g} are the radiative rates for transitions $2^3S_1-2^3P_{2,0,1}$ and $1^1S_0-2^3P_1$. The terms n_g and n_m , the absolute He-like ion ground and metastable popula-

tions (cm^{-3}), can be determined by considering all rates into and out of the triplet states, as described by Brenning for helium [20]. Although estimates show that this metastable population n_m is everywhere less than $10^{-4} n_g$ in the $TJ-I$ plasma, it is still included because excitation rates from this level are several orders of magnitude larger than those from the ground state. Therefore to estimate n_k , all terms on the right-hand sides of Eqs. (3) to (5) are required. For the moment it is assumed that all ion and neutral densities are well known, so the only unknowns are the CX rate coefficients $\sigma_k V_a$, since the C and A rates are widely available for low Z He-like ions.

C. Charge exchange partial cross sections

In order to determine separate rates for populating the 2^3P levels by cascades of electrons captured by CX, reliable l -level capture cross sections are needed, as well as knowledge of the branching ratios between intermediate l levels of the triplet manifold. Although total electron-capture cross sections are well established for low energy collisions of H-like ions with neutral hydrogen [21], experimental results on the n -state and l -level partial capture cross sections are scarce. For instance, in the case of C VI, Kimura *et al.* [22] show that the most likely capture state in CV is $n=4$, and not $n=3$ as predicted by the classical model $n=Z^{0.75}$, where Z is the charge on the ion [23]. Shimakura *et al.* [24] estimate the partial cross sections of C VI for energies from meV's to keV's per amu using quantum-mechanical and semiclassical molecular-orbital methods. They predict that the dominant capture channels in the triplet manifold of CV are $(1s4p)$, $(1s4d)$, and $(1s3p)$ above 0.1 keV/amu, while below this $(1s4s)$, $(1s4p)$, and $(1s4d)$ are dominant, with the capture cross section for $(1s4s)$ at least an order of magnitude larger than that for the other two levels. To date the partial cross sections for low energy collisions have not been substantiated by measurements, so reliance here is placed on the theoretical estimates. However, their values for total CX cross sections are in good agreement with the measurements of Phaneuf *et al.* [21].

While cross sections provide the populations of a given level by direct charge exchange events, the cascade process that follows electron capture can be significantly affected by the plasma environment. Although ionization from excited states tends to be unimportant for a tokamak plasma, processes that can be significant are l mixing in upper states due to collisions and to the motional Stark effect. Applying curves produced by Fonck, Darrow, and Jaehnic [25] to $TJ-I$ conditions, where $N_e < 5 \times 10^{13} \text{ cm}^{-3}$ and the magnetic field is 1.2 T, we predict that these l -mixing processes are only significant for n states greater than 5 for carbon and 6 for oxygen. Since direct capture into n states greater than 5 is negligible for these ions, this effect can be neglected here [24]. Also direct capture cross sections for 2^3S and 2^3P are negligible, so by following the procedure outlined by Fonck, Darrow, and Jaehnic [25], the cascade corrected emission cross sections σ_k for the 2^3P levels are estimated by using

$$\sigma_2 = \sigma(3s) + 0.55\sigma(3d) + 0.55\sigma(4s) \\ + 0.21\sigma(4p) + 0.43\sigma(4d) + 0.55\sigma(4f), \quad (6)$$

$$\sigma_1 = 0.33\sigma(3d) + 0.023\sigma(4p) \\ + 0.26\sigma(4d) + 0.33\sigma(4f), \quad (7)$$

$$\sigma_0 = 0.11\sigma(3d) + 0.008\sigma(4p) \\ + 0.09\sigma(4d) + 0.11\sigma(4f). \quad (8)$$

Here the partial cross sections for the triplet manifold, denoted by $\sigma(3s)$ etc., are found in Shimakura *et al.* [24] and the branching ratios are by Surard *et al.* [17]. The semiclassical partial cross sections therein apply to collisions with energies above 10 eV/amu. Partial cross sections below this are estimated using quantum-mechanical total cross sections and the relative magnitudes of the cross sections at 10 eV/amu. Applying the values in Table I to Eqs. (3)–(5), we can see that the 2^3P_2 level can be favorably populated at the expense of the other levels. This is because the $\Delta n = 2$ transitions from the then dominant electron-capture level $4s^3S$ populate only the 2^3P_2 level, while transitions from $4d^3D$ populate the three triplet levels according to their statistical weights [17]. In addition, cascades from $4p^3P$, which decay via the $3s^3S$ level, populate only the 2^3P_2 level, while cascades from $4p^3P$ and $4f^3F$ via the $3d^3D$ level populate the $2^3P_{2,0,1}$ levels, again according to their statistical weights. The argument is further strengthened when the CX emission rates for the 2^3P_2 level in Table II are compared with, and found to be equal to or greater than, those for the 2^3P_1 and 2^3P_0 levels and the electronic excitation rates from the ground and metastable states of C V [26]. Also, when these rates are compared with those for dielectronic and radiative recombination from C VI, it is seen that cascades originating from the recombination processes are several orders of magnitude less than those from CX [27,28]. Thus in Eqs. (3)–(5), the terms R_k^* can be dropped. Having determined that CX can compete with electron excitation, it is interesting to note how the population ratios of the 2^3P levels can change under different conditions. In the first instance, when $N_e[n_g C_{gk} + n_m C_{mk}] > N_0 N_h \sigma_k V_a$, the only process to work against a statistical distribution among the 2^3P levels is A_{1g} . In contrast, when CX dominates, the ratio n_2/n_1 approaches $1.5\sigma_2/\sigma_1$, while $n_2/(n_1+n_0)$ ap-

TABLE I. Estimated cascade corrected emission cross sections, σ_k (10^{-15} cm²), for the He-like carbon $2^3P_{2,0,1}$ levels in collisions between H-like carbon ions and neutral hydrogen atoms.

Collision strength (eV/amu)	σ_2	σ_1	σ_0
1	3.1	0.123	0.042
5	2.9	0.122	0.042
10	2.5	0.12	0.041
15	2.2	0.12	0.041
25	1.92	0.124	0.043
100	1.15	0.14	0.046

TABLE II. Estimated emission rates, $\delta_k \times V_a$ (10^{-8} cm³ s⁻¹), for the $2^3P_{2,0,1}$ levels of He-like carbon in collisions between H-like carbon and neutral hydrogen in the *TJ-I*.

Collision strength eV/amu	$\delta_2 \times V_a$	$\delta_1 \times V_a$	$\delta_0 \times V_a$
1	1.55	0.061	0.021
5	1.55	0.065	0.023
10	1.45	0.07	0.024
15	1.36	0.074	0.026
25	1.33	0.086	0.03
100	1.26	0.153	0.051

proaches $\sigma_2/(0.67\sigma_1 + \sigma_0)$. After showing that the population distribution among levels can vary over a wide range, it remains to be seen if this gives rise to the anomalies observed. In the next section a model is described that incorporates CX and re-creates the results obtained.

IV. APPLICATION OF MODEL

The model outlined here, which is based on Eqs. (3)–(5), has been developed to simulate the line of sight measurements through the *TJ-I* plasma. In order to avoid extensive numerical calculations when estimating the relative intensities of the $2^3S_1 - 2^3P_{2,0,1}$ emission lines in the model, the plasma was partitioned into many narrow and discrete circular concentric shells, and within each the plasma electron temperature and density were assumed constant. The profiles used here for these parameters are shown in Fig. 4 [29]. The C V distribution in each shell was determined from the measured 2271.59 Å line intensities shown in Fig. 2(a). The ground state and metastable populations, n_g and n_m , were estimated by considering the excitation, deexcitation, and ionization rates into and out of the triplet manifold [20]. The rate coefficients used are based on Maxwellian-type electron collision coefficient curves from Itikawa *et al.* [26] and on Maxwellian based equations described by Engelhardt, Köppendörfer, and Sommer [11]. For charge exchange,

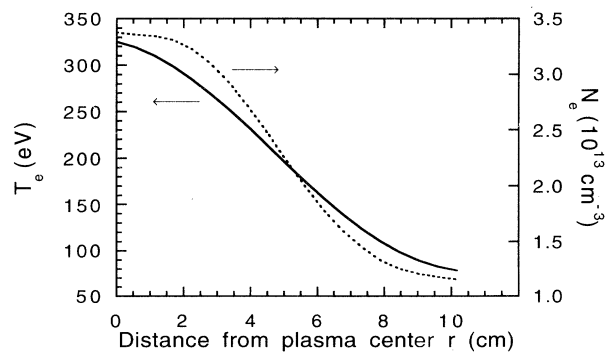


FIG. 4. Electron density and temperature profiles used in modeling *TJ-I* line of sight measurements. The curves are based on standard *TJ-I* profiles [29], which have been scaled using an experimental line averaged electron density measured through the plasma center, i.e., $2 - 2.5 \times 10^{13}$ cm⁻³.

the cascade corrected emission cross sections σ_k were estimated by using Eqs. (6)–(8). A constant temperature was assumed for the C VI ions (150 eV), even though the impurity temperature varies throughout the plasma. A fixed value can be used, since CX cross sections are almost constant for the range of C VI temperatures experienced in the *TJ-I*, typically 100–200 eV [14]. A fixed value for the neutral temperature (25 eV) was also assumed throughout when using the standard ion thermal velocity formula to estimate the relative collision velocities V_a . The neutral hydrogen profile used was based on edge source distributions from similar tokamaks [13]. The profile was scaled using a central neutral density value typical of the *TJ-I* and of a similar machine [14,30], i.e., 3 to $6 \times 10^9 \text{ cm}^{-3}$. This profile was then combined with a profile for C VI, which was best guessed in the first instance but altered, after several iterations of the model, by repeated modification to best fit the modeled *R* curves to measured data. Finally, using these parameters, the 2^3P level populations n_k were estimated for each shell in the model using Eqs. (3)–(5).

With the plasma parameters determined, the model continues by summing the 2^3P level populations along each line of sight path through the plasma. Starting at the plasma center and continuing to the plasma edge, the n_k populations for each 2^3P level were summed for equispaced paths according to $\sum n_k \Delta z$, where Δz is the length of shell intersected by the path. In reality this path has a width 1.5 cm, and so summations were made and averaged along three separate paths within this width. The intensities for each line of sight were determined using $A_{km} \sum n_k \Delta z$ and were used to create the curves shown in Fig. 2. Note that, as stated before, the curve for the ratio *R* in Fig. 2(b) was achieved by repeated corrections to the C VI and neutral hydrogen radial profile until a good fit to the data was obtained. The resultant radial profile is shown in Fig. 5. It should be noted here that, while $N_e \sum C_{kj} \ll A_{km}$ in Eqs. (3)–(5), the ratio $n_2/(n_1+n_0)$ can be determined using only the relative concentrations of the participating species. Thus relative concentrations can be used in Fig. 5. To determine if the C VI to C V ratio in Fig. 5 is reasonable, we

use the central electron and neutral hydrogen concentrations to make an estimation. At first this ratio, which is between 1 and 2.5, would appear to be in disagreement with the carbon corona model of Breton, Michelis, and Mattioli [31]. However, their model did not include charge exchange recombination, which can significantly increase the relative C V to C VI concentration [32]. This ratio also appears to be reasonable across the plasma, thus supporting the proposition that CX is the mechanism responsible for the anomalies seen. This hypothesis is in agreement with that of both Källne, Källne, and Pradhan [7] and Hess *et al.* [8]. Finally, when H-like ion concentration profiles are available, it is apparent that the neutral hydrogen atom concentrations could then be determined using the equations and the model described.

A. Sensitivity

While the sensitivity of the technique proposed may be ultimately dependent on good diagnostic techniques and on knowledge of the distribution profiles of the other plasma constituents, it is useful to make some estimates about the lowest neutral densities that might cause variations in the line ratios. Since the line intensities are directly related to the 2^3P level populations, it is reasonable to compare the populations among these levels. Thus, using the equations developed here, local 2^3P level population distributions are shown in Fig. 6 for a range of neutral concentrations as a function of the plasma local electron temperature. A constant electron density is used, i.e., $1 \times 10^{13} \text{ cm}^{-3}$, while the C V and C VI densities are assumed to be equal throughout. The first approximation is good since this value is representative of the electron density in many plasma, although in normal plasmas it falls toward the edge. The second is made for convenience, but it may not be unreasonable, especially in the plasma center where CX recombination effects can increase the C V concentration. Therefore, it can be inferred from these curves, within reason, that in the *TJ-I* center the population distribution among the 2^3P levels is altered significantly when the local neutral atom density

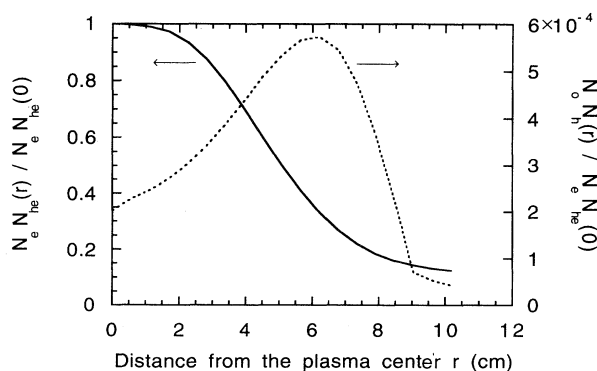


FIG. 5. Distribution of N_e/N_{he} and N_o/N_h across the *TJ-I* plasma radius relative to $N_e N_{he}$ at $r=0$. Here N_{he} refers to $(n_g + n_m)$.

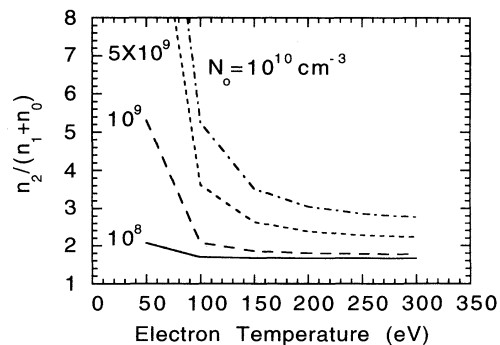


FIG. 6. The population distribution among the 2^3P levels in He-like carbon across the *TJ-I* plasma radius r as a function of neutral hydrogen concentration. The curves represent different neutral hydrogen concentrations (cm^{-3}) as indicated. Note that the electron density N_e and the C V and C VI concentrations are constant throughout.

N_0 is greater than 10^8 cm^{-3} . It should be noted, however, that Fig. 6 is slightly misleading for the plasma edge, where the concentration of C V is generally much larger than that of C VI. Thus the population distribution may be several orders of magnitude less sensitive there to neutral atoms than indicated here.

B. Other low Z He-like ions

The equations and model developed here could also be used to study similar transitions in other low Z He-like ions. While electron partial-capture cross sections for neutral hydrogen collisions have still to be determined for collisions with all the low Z ions, i.e., from B to Ne, some indications can be had from the data available. For instance, in the case of He-like boron (B IV), Shimakura, Suzuki, and Kimura [33] estimate that in the triplet manifold the $3p \ ^3P$ and $3d \ ^3D$ levels have the largest electron-capture cross sections. Since these levels cascade to populate the $2 \ ^3P_{2,0,1}$ levels according to their statistical weights, it is probable that the line emissions from these levels may be insensitive to the CX process and thus to neutral hydrogen concentrations. In contrast, the $4p \ ^3P$, $4d \ ^3D$, and $4f \ ^3F$ levels and the $5p \ ^3P$ level are the dominant capture levels in He-like nitrogen (N VI) and oxygen (O VII) [22]. Since their total capture cross sections are of the order 10^{-15} cm^2 [34], while branching ratios and decay routes indicate that the $2 \ ^3P_2$ level may be favorably populated at the expense of the other $2 \ ^3P$ levels, it appears that these $2 \ ^3P$ line emissions should be sensitive to the CX process and to neutral hydrogen concentrations, especially where electron temperatures may be several hundreds of electron volts. In the case of He-like neon (Ne IX), work to date has indicated that the singlet $6p \ ^1P$

level is the dominant capture level [22]. It may therefore be assumed that in the triplet manifold the $6p \ ^3P$ level is dominant, as also predicted by $n = Z^{0.75}$, thereby adding to the number of low Z ions whose $2 \ ^3P$ line emissions may be sensitive to neutral hydrogen atoms in plasmas. Finally, although variations have been seen in line ratios of S XV and Cl XVI [7] it may be difficult to establish if CX is the mechanism responsible for these anomalies until electron partial-capture cross sections become available for H-like sulfur and chlorine.

V. CONCLUDING REMARKS

We have shown that the process of charge exchange between H-like carbon ions and neutral hydrogen atoms, where electrons captured by high n states can selectively decay to one of the $2 \ ^3P$ levels of the He-like carbon ion, can compete with plasma electron excitation processes to create a nonstatistical population among the $2 \ ^3P$ levels. Having established, by use of equations and a model, that this process is responsible for the variations in the ratios of the $2 \ ^3P$ line intensities, we have proposed monitoring these emission lines as a means to estimate the concentration of neutral hydrogen atoms in plasmas. Finally, we extended the discussion to other low Z He-like ions and concluded that variations in the intensity ratios may be seen in the triplet line emissions of such ions.

ACKNOWLEDGMENTS

This work is supported by the Spanish Ministry of Science and Education and was partially funded by Project No. PB94-1229. K. J. McCarthy acknowledges financial support from the same organization.

-
- [1] L. Engström, P. Bengtsson, C. Jupén, and M. Westerlind, *J. Phys. B* **25**, 2459 (1992).
 - [2] P. Monier-Garbet, in *Diagnostics for Contemporary Fusion Experiments*, edited by P. E. Stott, D. K. Akulina, G. Gorini, and E. Sindoni (Editrice Compositori, Bologna, 1991), p. 331.
 - [3] C. D. Lin, W. R. Johnson, and A. Dalgarno, *Phys. Rev. A* **15**, 154 (1977).
 - [4] A. K. Pradhan and J. Michael Shull, *Astrophys. J.* **249**, 821 (1981).
 - [5] F. P. Keenan, in *Proceedings of the 10th International Colloquium on UV and X-ray Spectroscopy of Laboratory and Astrophysical Plasmas*, edited by E. H. Silver and S. M. Kahn (Cambridge University Press, Cambridge, 1993), p. 44.
 - [6] S. Suckewer and E. Hinnov, *Nucl. Fusion* **17**, 5 (1977).
 - [7] E. Källne, J. Källne, and A. K. Pradhan, *Phys. Rev. A* **27**, 1476 (1983).
 - [8] W. R. Hess, C. De Michelis, M. Mattioli, R. Guirlet, and M. Druetta, *Nucl. Instrum. Methods B* **98**, 97 (1995).
 - [9] W. L. Wiese, M. W. Smith, and B. M. Glennon, *Atomic Transition Probabilities*, Nat'l. Bur. Stand. (U.S.) Natl. Stand. Ref. Data Ser. No. 4 (U.S. GPO, Washington, D.C., 1966), Vol. 1.
 - [10] R. L. Kelly, *Atomic and Ionic Spectrum Lines below 2000 Ångströms: Hydrogen through Krypton*, special issue of *J. Phys. Chem. Ref. Data* **16**, Suppl. No. 1 (1987).
 - [11] W. Engelhardt, W. Köppendorfer, and J. Sommer, *Phys. Rev. A* **6**, 1908 (1972).
 - [12] Y. Chung, P. Lemaire, and S. Suckewer, *Phys. Rev. Lett.* **60**, 1122 (1988).
 - [13] R. C. Isler, *Phys. Scr.* **35**, 650 (1987).
 - [14] B. Zurro, C. Hidalgo, B. García-Castañer, and C. Pardo, *Plasma Phys. Contr. Fusion* **32**, 565 (1990).
 - [15] I. C. Percival and M. J. Seaton, *Philos. Trans. R. Soc. London* **251A**, 113 (1958).
 - [16] J. G. Doyle, *Astron. Astrophys.* **87**, 183 (1980).
 - [17] M. G. Surraud, R. Hoekstra, F. J. de Heer, J. J. Bonnet, and R. Morgenstern, *J. Phys. B* **24**, 2543 (1991).
 - [18] E. Källne, J. Källne, A. Dalgarno, E. S. Marmar, J. E. Rice, and A. K. Pradhan, *Phys. Rev. Lett.* **52**, 2245 (1984).
 - [19] R. Hutton, N. Reistad, L. Engström, and S. Huldt, *Phys. Scr.* **31**, 506 (1985).
 - [20] N. Brenning, *J. Phys. D* **13**, 1459 (1980).
 - [21] R. A. Phaneuf, I. Alvarez, F. W. Meyer, and D. H. Crandall, *Phys. Rev. A* **26**, 1892 (1982).
 - [22] M. Kimura, N. Kobayashi, S. Ohtani, and H. Tawara, *J. Phys. B* **20**, 3873 (1987).

- [23] R. E. Olson, *Phys. Rev. A* **24**, 1726 (1981).
- [24] N. Shimakura, S. Koizumi, S. Suzuki, and M. Kimura, *Phys. Rev. A* **45**, 7876 (1992).
- [25] R. J. Fonck, D. S. Darrow, and K. P. Jaehnig, *Phys. Rev. A* **29**, 3288 (1984).
- [26] Y. Itikawa, S. Hara, T. Kato, S. Nakazaki, M. S. Pindzola, and D. H. Crandall, Institute of Plasma Physics, Nagoya University, Report No. IPPJ-AM-27, 1983 (unpublished).
- [27] S. Bliman, M. Cornille, and K. Katsonis, *Phys. Rev. A* **50**, 3134 (1994).
- [28] M. S. Pindzola, N. R. Badnell, and D.C. Griffin, *Phys. Rev. A* **42**, 282 (1990).
- [29] C. Pardo, Ph.D. thesis, Universidad Complutense de Madrid, 1986 (unpublished).
- [30] G. Reinhold, J. Hackman, and J. Uhlenbusch, *J. Nucl. Mater.* **121**, 231 (1984).
- [31] C. Breton, C. De Michelis, and M. Mattioli, EURATOM-CEA Association, Fontenay-aux-Roses, Report No. EUR-CEA-FC 853, 1976 (unpublished).
- [32] R. C. Isler, *Plasma Phys. Contr. Fusion* **36**, 171 (1994).
- [33] N. Shimakura, S. Suzuki, and M. Kimura, *Phys. Rev. A* **47**, 3930 (1993).
- [34] H. Tawara, T. Kato, and Y. Nakai, Institute of Plasma Physics, Nagoya University, Report No. IPPJ-AM-30, 1983 (unpublished).